Hindawi
Geofluids
Volume 2023, Article ID 7898356, 14 pages
https://doi.org/10.1155/2023/7898356

*Research Article*

# Differential Occurrence Characteristics and Influence Factors of Reservoir Movable Fluids in Tight Gas: A Case Study of Shan 1 Reservoir in Yanchang Area

**Jiangbin Liu and Xiaobin Wu**

*Yan'an University, Yan'an 716000, China*

Correspondence should be addressed to Jiangbin Liu; liujiangbin@yau.edu.cn

Received 27 May 2022; Revised 1 September 2022; Accepted 19 September 2022; Published 21 March 2023

Academic Editor: Dengke Liu

Copyright © 2023 Jiangbin Liu and Xiaobin Wu. This is an open access article distributed under the Creative Commons Attribution License, which permits unrestricted use, distribution, and reproduction in any medium, provided the original work is properly cited.

The occurrence characteristic of movable fluid is a crucial index for tight sandstone reservoir evaluation, and the study of the differential occurrence of reservoir movable fluid is vitally important for the exploration and development of tight gas. Therefore, on the basis of casting thin section, scanning electron microscope, X-ray diffraction, high-pressure mercury injection, and nuclear magnetic resonance testing, the differential occurrence characteristics and influencing factors of reservoir movable fluid are analyzed based on the reservoir of Shan 1 reservoir. The results show that the main types of Shan 1 reservoir are lithic quartz sandstone and lithic sandstone, and intergranular solution pores and cutting solution pores are mainly developed in Shan 1 reservoir in Yanchang area. The movable fluid saturation of Shan 1 reservoir is 21.64%~69.62%, and the average of the movable fluid saturation is 35.32%. Most of the $T_2$ spectra are unimodal. According to the pore development, the reservoir is divided into four types, and fluid flow property in reservoir varies with the difference of reservoir pore development. Sandstone types, reservoir porosity, permeability, pore type, pore throat parameters, and cement content affect movable fluid saturation. The pores provide the main space for the movable fluid. The better the development of intergranular solution pores, the larger the average pore throat radius and the higher the movable fluid saturation of the reservoir. The higher the content of the calcite, the more obvious pore loss of the reservoir and the lower movable fluid saturation in the reservoir. The higher the content of illite, the worse the pore evolution and the lower fluid flow property in reservoir.

## 1. Introduction

Tight sandstone gas is an important field of unconventional natural gas exploration [1, 2]. Domestic tight sandstone gas fields are mainly distributed in Ordos Basin, Sichuan Basin, and Tarim Basin. The Upper Paleozoic tight sandstone gas in Ordos Basin plays an important role in production of tight gas of China, and it is the largest tight sandstone gas base in China. The Upper Paleozoic Shihezi Formation and Shanxi Formation are the main target strata for the study of tight gas. The producing degree of reserves in Shan 1 member is not high, but it is difficult to exploit and lack of understanding of fluid occurrence characteristics, which directly affects the production of tight gas of Shan 1 reservoir.

Tight reservoir has small pore size and extremely complex pore property [3–5]. The accurate description of reservoir pore structure has become the key content of tight reservoir research. At present, field emission scanning electron microscope, focused ion beam field emission scanning electron microscope, transmission electron microscope, CT scanning, gas adsorption, high-pressure/constant velocity mercury injection, and other technologies have effectively promoted the research process of pore structure in the tight reservoir. The constant velocity mercury injection

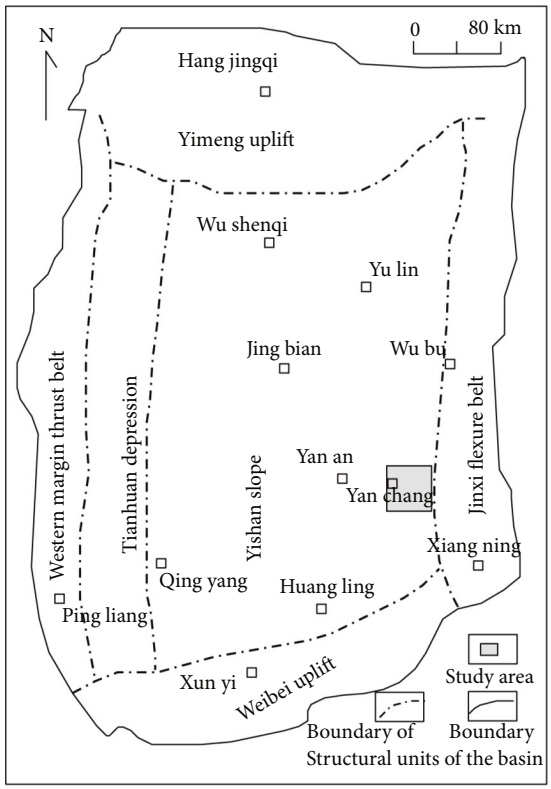


Figure 1: Structural location of Yanchang area in Ordos Basin.

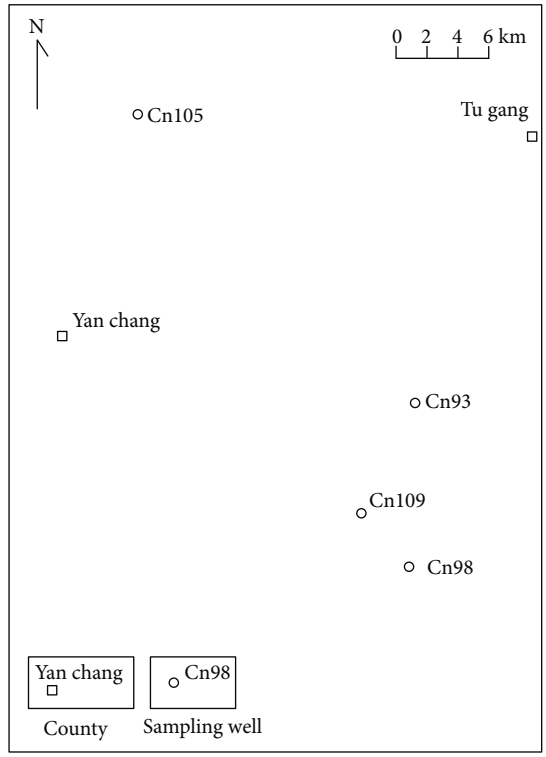


Figure 2: Location of sampling wells in Yanchang area.

technique has been well applied in the accurate analysis of pore and throat and has obvious advantages over conventional method [6–9]. The nuclear magnetic resonance method has the advantages of intuition and rapidity and has been well applied in evaluating the occurrence characteristics of movable fluids [10–14].

Affected by the difference of provenance supply and sedimentary environment, the diagenetic minerals of tight reservoir are different, so the pore development and diagenetic evolution are different in the type and evolution process, and the types of reservoir are also different. The different diagenetic facies, flow units, and rock types of the reservoir affect the pore structure of the reservoir, and the difference of pore structure further affects the differential distribution of movable fluids [15–17]. It is considered that pore structure, permeability, clay minerals, development of secondary pores, compaction, and other factors affect movable fluid [18, 19]. However, the differential occurrence of movable fluids, especially the mechanism of differential occurrence of movable fluids in reservoirs with different pore structures, still needs to be further studied.

At present, there are few studies on the occurrence characteristics of movable fluids in Shan 1 reservoir of Ordos Basin. The lack of understanding of the differential occurrence of movable fluids directly affects the exploration and production of tight gas. Therefore, the typical area in Ordos Basin is selected as the research object, through multiple experimental methods. Pore property and movable fluid occurrence characteristics of the reservoir are analyzed, and the differential occurrence of movable fluid and its influencing factors are studied to accurately and effectively identify the reservoir and provide guidance for the exploitation of tight sandstone gas in Ordos Basin.

## 2. Overview of Regional Geology

After a long epoch of erosion, Ordos Basin entered late Paleozoic period [20], and the influence of transgression was gradually weakened. Ordos Basin transformed into continental environment. The provenance supply increased in the north of Ordos Basin during the sedimentary period of Shanxi formation. Fluvial facies, delta facies are developed successively [21, 22]. The delta front deposits developed in Yulin Zizhou area during the Shanxi period [23], and the delta front extended southward to Yanchang area. The Yanchang area is located in the slope of northern Shaanxi (Figure 1). The Shanxi Formation is divided into Shan 2 and Shan 1 from bottom to top. Shan 1 is an important gas-producing section in Yanchang area. The formation thickness of Shan 1 in Yanchang area is 42-58 m. Grey coarse sandstone, medium sandstone, and fine sandstone are developed, mudstone is dark gray, and thin carbonaceous mudstone and coal seam can be seen. There are trough-like cross-bedding, plate-like cross-bedding, and parallel bedding in sandstone, and plant detritus is common in mudstone. According to the electrical characteristics, the underwater distributary channel and interdistributary bay microfacies are divided. Among them, the underwater distributary channel sand body is the skeleton sand body of

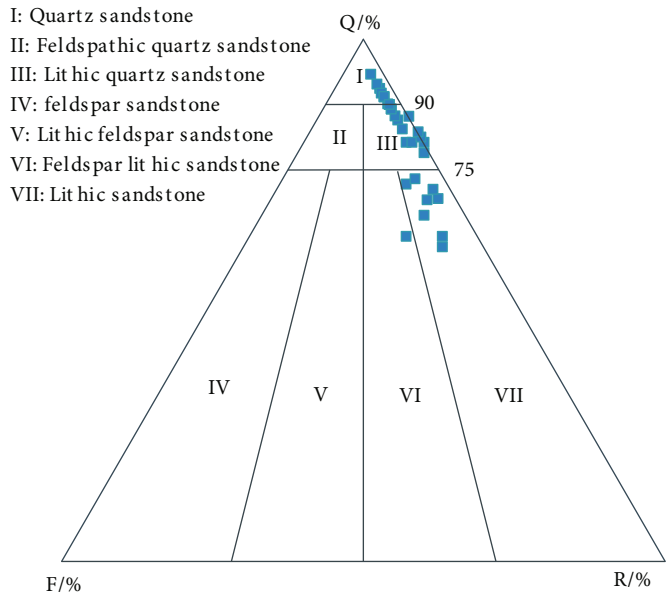


Figure 3: Reservoir petrology types of Shan 1 in Yanchang area.

Table 1: Mineral content of Shan 1 reservoir in Yanchang area.

| Mineral content | Quartz (%) | Feldspar (%) | Volcanic cuttings (%) | Metamorphic cuttings (%) | Sedimentary cuttings (%) | Other (%) |
|---|---|---|---|---|---|---|
| Maximum value | 93.91 | 18.00 | 34.00 | 20.00 | 35.00 | 25.00 |
| Minimum value | 45.00 | 0.00 | 0.00 | 2.00 | 0.00 | 0.00 |
| Average value | 75.80 | 2.31 | 7.01 | 11.11 | 1.30 | 2.47 |

the study area, and several underwater distributary channels are developed, with a channel width of 2~4 km. The sand bodies are staggered and superimposed and distributed in a large area on the plane.

## 3. Samples and Methods

In this study, coring sections of Shan 1 member such as Cn98 well, Cn105 well, and Cn93 well are selected in the sample Yanchang area (Figure 2). The samples were tested by casting thin section, scanning electron microscope, high-pressure mercury injection test, XRD test, and nuclear magnetic resonance experiment. The epoxy resin casting slices were made according to the national standard and identified and analyzed by polarizing microscope 59XC-PC. The samples were divided, prepared, and sprayed with gold, and the samples were tested and analyzed by FEI Quanta 450FEG scanning electron microscope under the condition of accelerated voltage 500-30 kV. The samples were analyzed by AutoPore IV 9500 high-pressure mercury porosimeter. The samples were washed with oil, dried, crushed, and ground, and the films were made. The relative contents of whole rock and clay minerals were quantitatively analyzed by X-ray diffractometer/YST-I test diffraction peak. The nuclear magnetic resonance samples were analyzed by MesoMR-12-040H nuclear magnetic resonance analyzer. After sample preparation and saturated formation water (salinity is 53236 ppm), $T_2$ spectrum was tested and then centrifuged under the condition of 2.07 MPa (300 psi) according to the industry standard. $T_2$ relaxation time cutoff value was obtained, and movable fluid saturation was calculated.

## 4. Results

### 4.1. Characteristics of Reservoir Pore Development

*4.1.1. Petrology and Pore Types.* The reservoir main petrology types of Shan 1 member of Shanxi formation in Yanchang area are lithic quartz sandstone and rock fragment sandstone (Figure 3), followed by quartz sandstone. The specific mineral content is shown in Table 1. The sandstone is mainly medium-sized, subedge-subcircular, the particles are well sorted, and the cementation is pore cementation. Clay minerals are the main cements (Figures 4(i), 4(j), and 4(l)), followed by calcite, iron calcite, and a small amount of siliceous. The results of scanning electron microscope and X-ray diffraction (XRD) show that the clay mineral is mainly illite, the second is kaolinite, and the content of chlorite is less. Illite is filamentous and hairy and filled in intergranular pores (Figures 5(b), 5(c), and 5(f)). Kaolinite is in the shape of a page (Figures 5(f) and 5(i)), with intercrystalline pores and local illite. Chlorite is leaf-shaped and regular in shape (Figures 5(c), 5(d), and 5(g)). It is mostly attached to the particles, and authigenic quartz can be seen in the area where it occurs with illite. Calcite is cemented in monocrystalline type (Figures 5(h) and 5(i)). The main pores types are

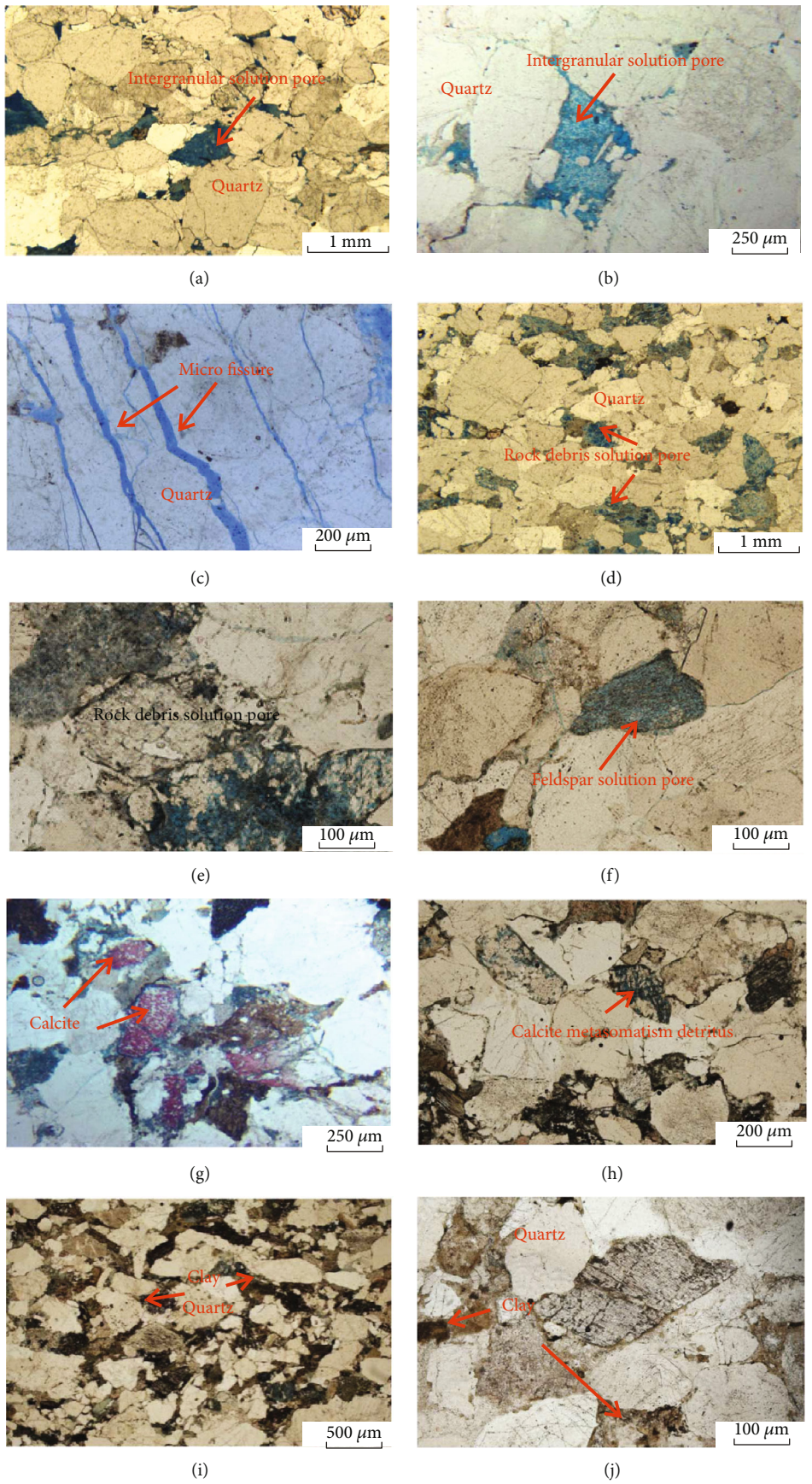


Figure 4: Continued.

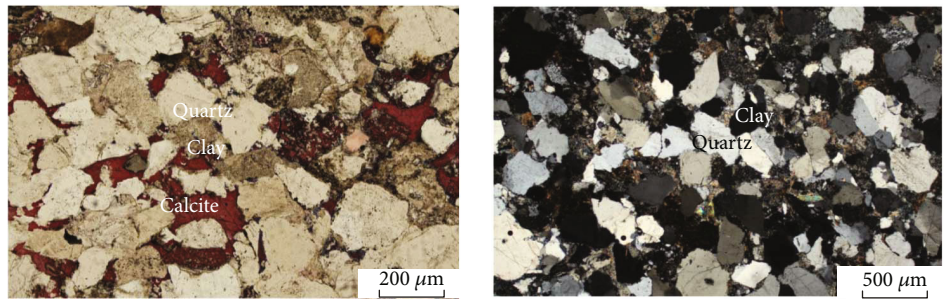


(k) (l)

Figure 4: Pore characteristics of Shan 1 reservoir. (a) Intergranular solution pore, Cn105 well, 2482.84 m. (b) Intergranular solution pore, Cn109 well, 2221.37 m. (c) Microfissure, Cn93 well, 2276.68 m. (d) Rock debris solution pore, Cn105 well, 2488.78 m. (e) Rock debris solution pore, Cn98 well, 2087.1 m. (f) Feldspar solution pore, Cn98 well, 2096.18 m. (g) Calcite cementation, Cn98 well, 2093.71 m. (h) Calcite metasomatism detritus, Cn98 well, 2091.46 m. (i) Clay mineral filling pore, Cn98 well, 2091.9 m. (j) Clay mineral filling pore, Cn98 well, 2093 m. (k) Calcite cementation and clay mineral filling, Cn98 well, 2094.46 m. (l) Quartz secondary enlargement and clay mineral filling, Cn98 well, 2095.42 m.

mainly intergranular solution pores and rock debris solution pores, followed by intergranular pores (Figure 4). There are few microfissures. The reservoir porosity is 1.03%-14.55%; the reservoir permeability is $0.01 - 15.20 \times 10^{-3}\ \mu m^2$. There is a good correlation between reservoir porosity and permeability, and microfractures are not developed, which has the characteristics of porous reservoir [24, 25].

*4.1.2. Pore Structure Types.* Through the analysis of experimental result, the reservoir is divided according to the difference of pore development by comprehensive reservoir casting thin section and scanning electron microscope test (Figure 6, Table 2), which can be divided into four types.

Type I reservoirs are mainly characterized by intergranular solution pores and rock debris solution pores (Figures 4(a)–4(c)). The content of intergranular solution pores is about 1%~5%, and the content of cuttings solution pores is about 1%~4%. Microfissures can still be seen. The cements are mainly kaolinite and siliceous. The porosity is 6.30%~14.55%; the permeability is $0.02 \sim 1.72 \times 10^{-3}\mu m^2$. The capillary pressure curve has a slow stage (Figure 6), the threshold pressure is 0.33~1.45 MPa, the average threshold pressure is 0.71 MPa, and the maximum connected pore radius is 0.52~2.22 $\mu$m; maximum mercury saturation is 73.14%~88.3%, with an average of 81.26%. Relative separation coefficient is between 1.52 and 5.65, and microfissures may aggravate the pore heterogeneity.

Type II reservoirs are mainly composed of rock debris solution pores and intergranular solution pores (Figures 4(d)–4(f)). The content of dissolution pores is about 1% to 8%, and the content of intergranular solution pores is about 1% to 2%. The cements are mainly illite, kaolinite, and siliceous. The porosity is 2.18%~10.63%; the permeability is $0.03 \sim 0.31 \times 10^{-3}\mu m^2$. There is a smooth segment in mercury inflow curve, and the mercury saturation is relatively high (Figure 6). The threshold pressure is 0.67~23.86 MPa; the maximum mercury saturation is 48.67%~83.83%.

Lithic solution pores are mainly developed in type III reservoir, intergranular solution pores are less, and a small amount of feldspar solution pores can be seen (Figures 4(g)–4(i)). The cements are mainly siliceous, illite, and kaolinite. Calcite cementation can be seen in the thin section, and the pore development is poor. The porosity is 2.61%~5.5%, with an average of 3.93%; the permeability is $0.05 \sim 0.15 \times 10^{-3}\mu m^2$, with an average of $0.08 \times 10^{-3}\mu m^2$. There is a short gentle segment in mercury inflow curve and the mercury saturation is relatively low (Figure 6). The threshold pressure is 1.57~21.59 MPa; the maximum mercury saturation is 46.35%~66.24%.

The pore development of type IV reservoir is extremely poor, showing that the pores are filled by calcite and muddy, mainly micropores (Figures 4(j)–4(l)). Illite and calcite are the main cements, followed by siliceous and siderite. The content of argillaceous detritus is between 7% and 18%. Clay mineral content of whole rock analysis of XRD can reach 26.7%. There is no smooth segment of the mercury intake curve, which is characterized by low mercury saturation (Figure 6). The porosity is 2.11%~3.55%, with an average of 2.63%; the permeability is $0.04 \sim 0.15 \times 10^{-3}\mu m^2$, with an average of $0.09 \times 10^{-3}\mu m^2$. The threshold pressure is 3.43~65.85 MPa; the maximum mercury saturation is 23.06%~27.65%, with an average of 25.32%; the relative separation coefficient is 2.64~3.36, and the pore throat difference is obvious.

*4.2. Differential Occurrence Characteristics of Reservoir Movable Fluid.* Nuclear magnetic resonance studies the relaxation spectrum ($T_2$ spectrum) of relaxation time and then analyzes the characteristics of reservoir pores and fluids. $T_2$ relaxation time is closely related to pore size [26]. $T_2$ relaxation time cutoff is an important parameter to distinguish movable fluid from bound fluid [12]. The intensity information of relaxation time is processed as porosity component parameters, as shown in Figure 7 and Table 2. The sample test data show that the $T_2$ relaxation time cutoff value of Shan 1 reservoir is between 0.44 and 8.33 ms, and the movable fluid saturation is 21.64%~69.62%, with an average of 35.32%.

The $T_2$ spectrum shape of Shan 1 reservoir can be divided into unimodal type and bimodal type, mainly unimodal type (Figure 7). The reservoir movable fluid saturation

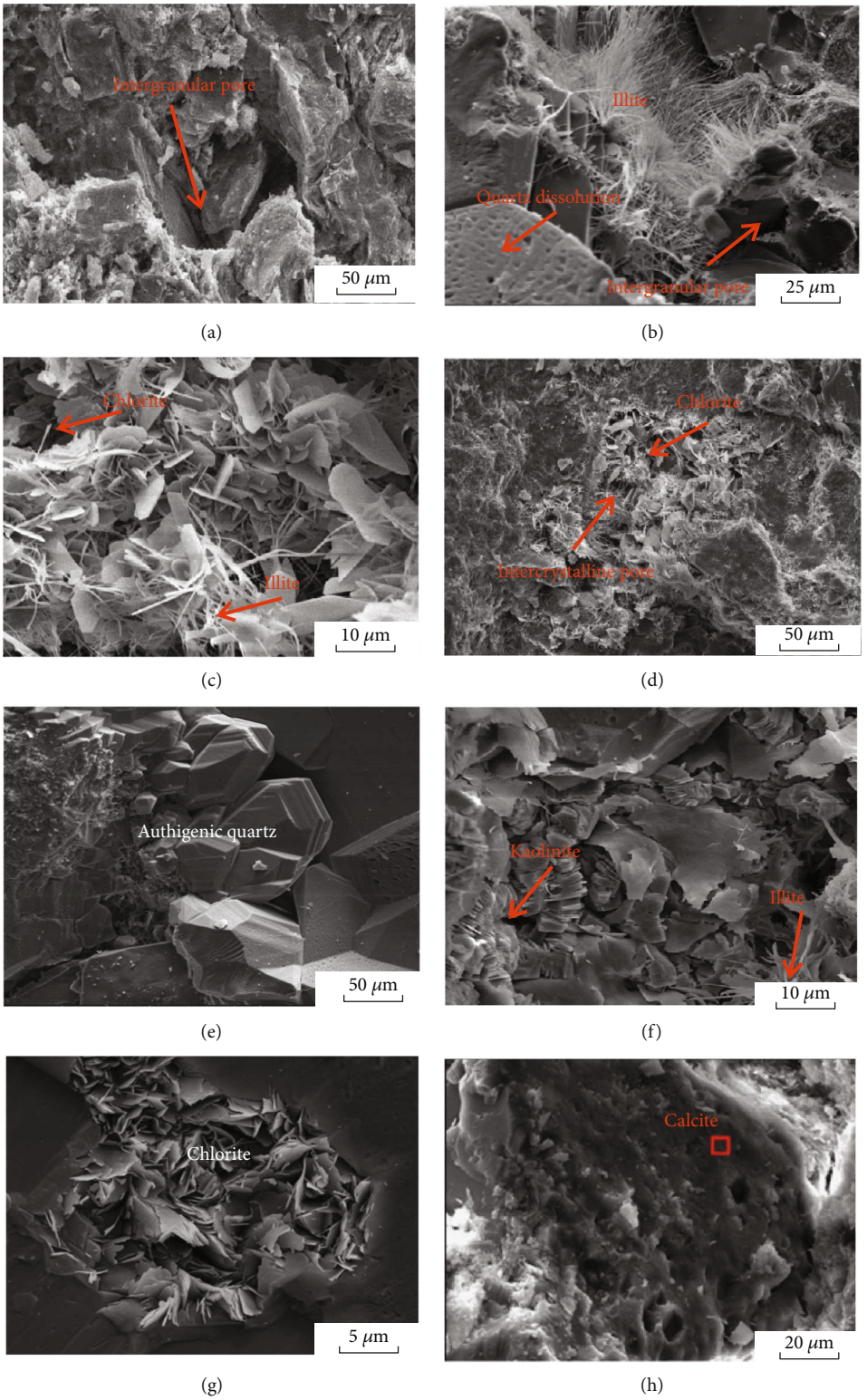


Figure 5: Continued.

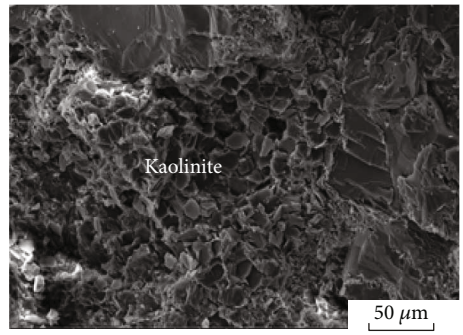


(i)

Figure 5: Pictures of pore and cement in scanning electron microscope. (a) Intergranular pore, Cn109 well, 2221.37 m. (b) Illite and quartz dissolution, Cn105 well, 2482.84 m. (c) Illite and chlorite, Cn105 well, 2482.99 m. (d) Chlorite and intercrystalline pore, Cn93 well, 2276.68 m. (e) Authigenic quartz, Cn105 well, 2483.14 m. (f) Kaolinite and illite, Cn105 well, 2483.14 m. (g) Chlorite, Cn105 well, 2487.58 m. (h) Calcite, Cn105 well, 2487.26 m. (i) Kaolinite, Cn 98 well, 2091.57 m.

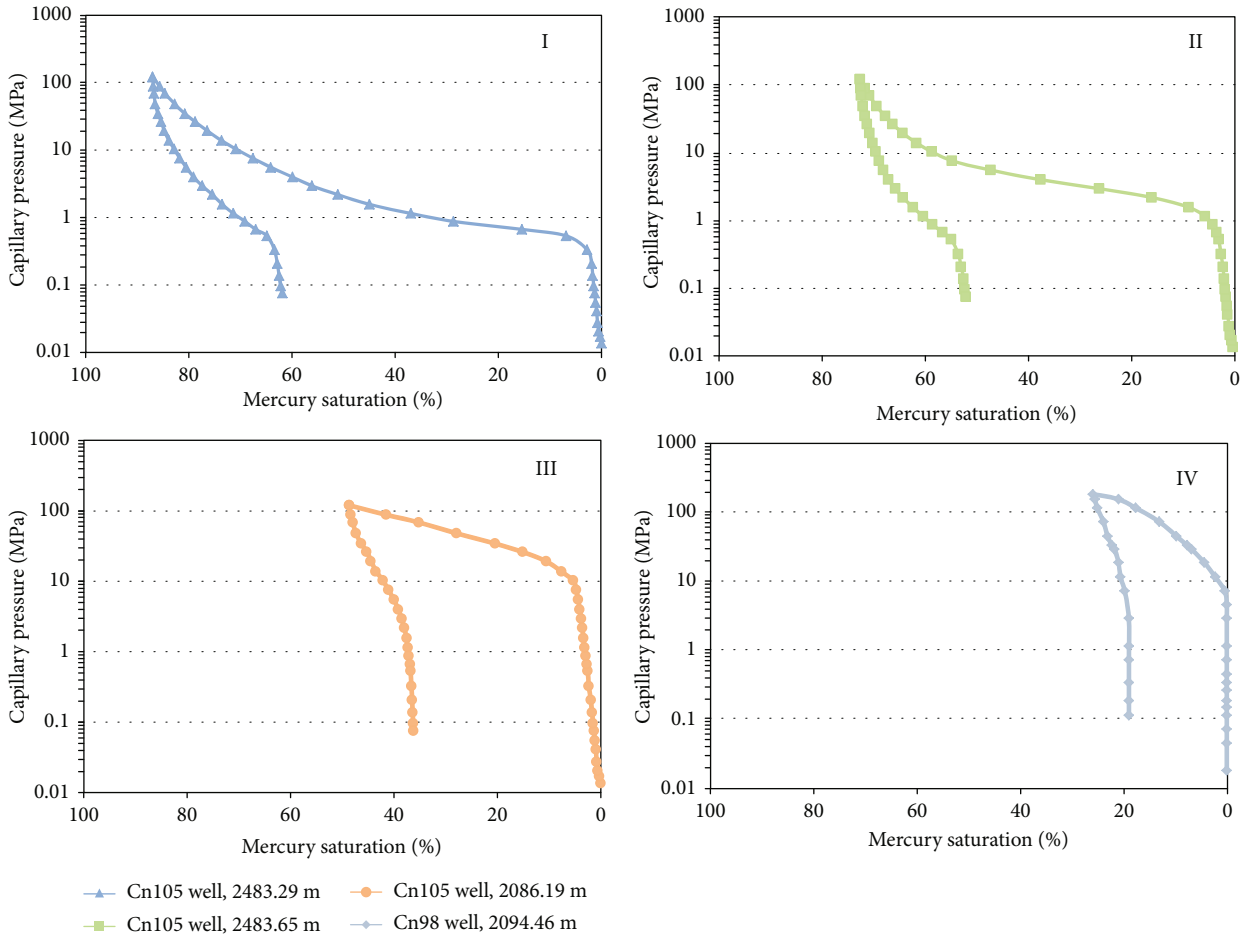


Figure 6: Capillary pressure curve characteristics of different types of reservoir.

of type I reservoir is 64.45%~69.62%, the average is 67.04%, the $T_2$ spectrum is bimodal, and the right peak is the main peak; the movable fluid saturation of type II reservoir is 21.64%~47.35%, the average is 34.48%, the $T_2$ spectrum is unimodal, the movable fluid saturation of type III reservoir is 27.78%~36.64%, and the average is 32.58%. The saturation of type IV reservoir movable fluid is 25.39%-34.94%, with an average of 29.69%. The $T_2$ spectrum is unimodal.

## 5. Discussion

The dissolution pores of Shan 1 member in Yanchang area are developed, the intergranular pores are preserved to a certain extent, the influence of microfractures is not obvious, and the reservoir properties are relatively good. The factors affecting the occurrence of movable fluid are discussed in the following sections.

Table 2: Capillary pressure parameters and fluid flow property in reservoir.

| Reservoir classification | Porosity (%) | Permeability ($10^{-3}$ $\mu$m) | Displacement pressure (MPa) | Median saturation pressure (MPa) | Maximum pore radius ($\mu$m) | Average pore radius ($\mu$m) | Median pore radius ($\mu$m) | Maximum mercury saturation (%) | Sorting coefficient | Movable fluid saturation (%) |
|---|---|---|---|---|---|---|---|---|---|---|
| I | | | | | | | | | | |
| Maximum value | 14.55 | 1.72 | 1.45 | 5.11 | 2.22 | 0.77 | 0.56 | 88.30 | 5.65 | 69.62 |
| Minimum value | 6.30 | 0.02 | 0.33 | 1.35 | 0.52 | 0.33 | 0.14 | 73.14 | 1.52 | 64.45 |
| Average value | 9.08 | 0.39 | 0.71 | 2.88 | 1.26 | 0.50 | 0.31 | 81.26 | 2.97 | 67.04 |
| II | | | | | | | | | | |
| Maximum value | 10.63 | 0.31 | 23.86 | 159.08 | 1.10 | 0.35 | 0.20 | 83.83 | 7.08 | 47.35 |
| Minimum value | 2.18 | 0.03 | 0.67 | 3.72 | 0.03 | 0.02 | 0.01 | 48.67 | 1.30 | 21.64 |
| Average value | 6.94 | 0.19 | 3.23 | 23.31 | 0.50 | 0.16 | 0.09 | 70.81 | 1.97 | 34.48 |
| III | | | | | | | | | | |
| Maximum value | 5.50 | 0.15 | 21.59 | 131.71 | 0.47 | 0.11 | 0.02 | 66.24 | 4.47 | 36.64 |
| Minimum value | 2.61 | 0.05 | 1.57 | 45.27 | 0.03 | 0.02 | 0.01 | 46.35 | 1.34 | 27.78 |
| Average value | 3.93 | 0.08 | 6.36 | 80.14 | 0.19 | 0.07 | 0.01 | 54.29 | 2.24 | 32.58 |
| IV | | | | | | | | | | |
| Maximum value | 3.55 | 0.15 | 65.85 | / | 0.21 | 0.07 | / | 27.65 | 3.36 | 34.94 |
| Minimum value | 2.11 | 0.04 | 3.43 | / | 0.01 | 0.07 | / | 23.06 | 2.64 | 25.39 |
| Average value | 2.63 | 0.09 | 30.69 | / | 0.10 | 0.07 | / | 25.32 | 2.96 | 29.69 |

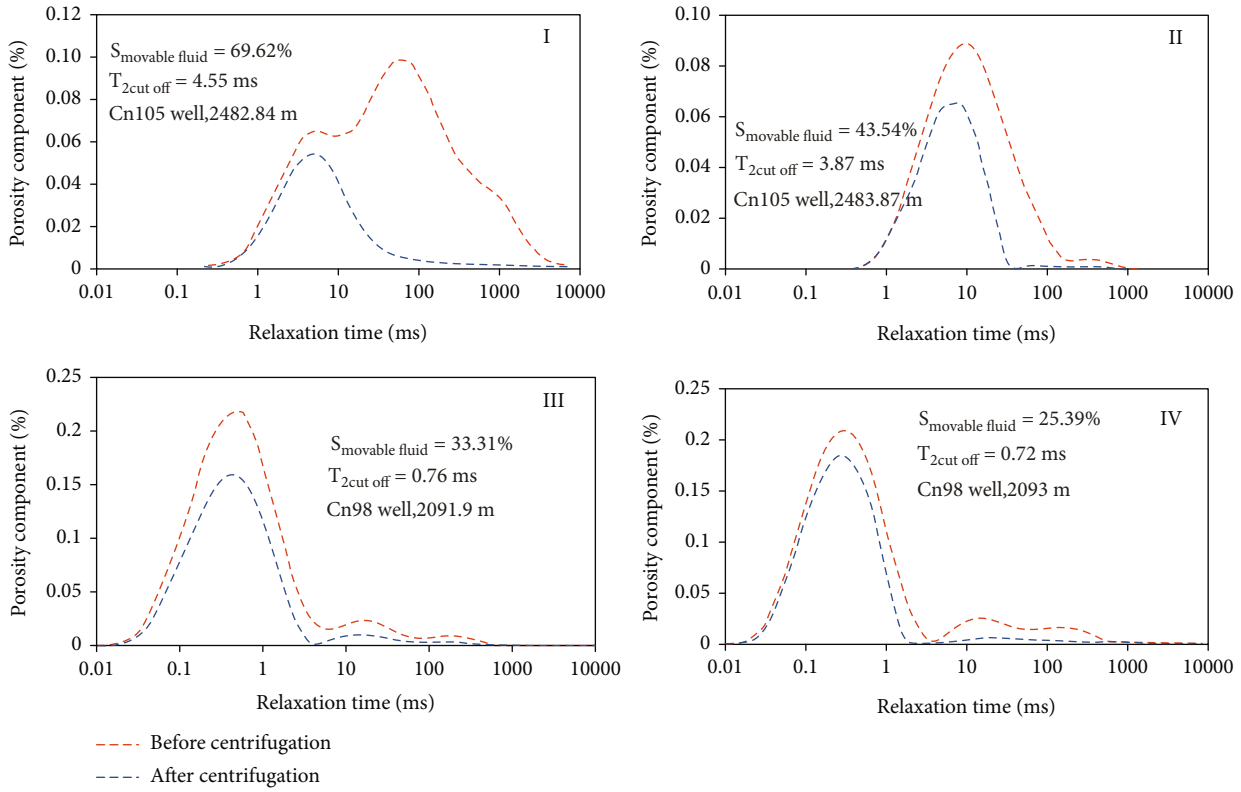


Figure 7: $T_2$ spectrum distribution of Shan 1 reservoir in Yanchang area.

*5.1. Petrology Types.* The movable fluid saturation of different sandstone types is shown in Table 3. Different mineral composition of sandstone will lead to different pore development during diagenesis [27], while quartz sandstone and lithic quartz sandstone can resist compaction so that the early pores can be preserved, and some pores remain in the middle stage of fluid transformation, so they have better physical properties and the movable fluid saturation is relatively high. On the other hand, the lithic sandstone, especially the higher the content of mudstone cuttings, the easier it is to be squeezed and the compaction is obvious, resulting in poor pore development, which is not conducive to fluid flow.

*5.2. Reservoir Physical Properties.* The physical property of the reservoir is the reflection of the macroscopic properties of the reservoir. Porosity and permeability reflect the reservoir property and permeability, respectively, which is the concentrated embodiment of the quality of the reservoir. As shown in Figure 6, there is a good positive correlation between reservoir porosity and permeability and movable fluid saturation. The results show that the better the reservoir porosity and permeability, the higher the movable fluid saturation of the reservoir. However, when the permeability is below $0.5 \times 10^{-3}$ $\mu m^2$, the correlation between permeability and movable fluid saturation increases. There is a high correlation between porosity and movable fluid, which reflects that macropores are beneficial to fluid flow, and there is a good correlation between porosity and permeability, which is related to that the reservoir is less affected by microfractures.

Table 3: Movable fluid saturation of different sandstone reservoirs.

| Movable fluid saturation (%) | Quartz sandstone | Lithic quartz sandstone | Lithic sandstone |
|---|---|---|---|
| Maximum value | 69.62 | 47.35 | 36.64 |
| Minimum value | 21.72 | 21.64 | 25.39 |
| Average value | 44.96 | 34.92 | 31.35 |

*5.3. Reservoir Pore Throat Parameters.* Intergranular solution pores and cutting solution pores are the main pore types of Shan 1 member in Yanchang area. The analysis of the relationship between intergranular solution pores, cutting solution pores, and movable fluid saturation is shown in Figures 8(c) and 8(d). The intergranular solution pores and cutting solution pores are positively correlated with saturation of movable fluid, and there is a good correlation between intergranular solution pores and movable fluid saturation, and the correlation coefficient can reach 0.4893, indicating that the more developed intergranular solution pores, the higher the movable fluid saturation. The thin section of the casting shows that the reservoirs with intergranular solution pores are mostly developed with pores and small throats, and the higher the area porosity is, the more favorable the fluid flow is. The thin section of the casting shows that the development of rock debris solution pores is dispersed and smaller than that of intergranular solution pores, and the development of throat is smaller, so the more developed rock debris solution pores, the higher the corresponding movable fluid saturation, but the effect is not as

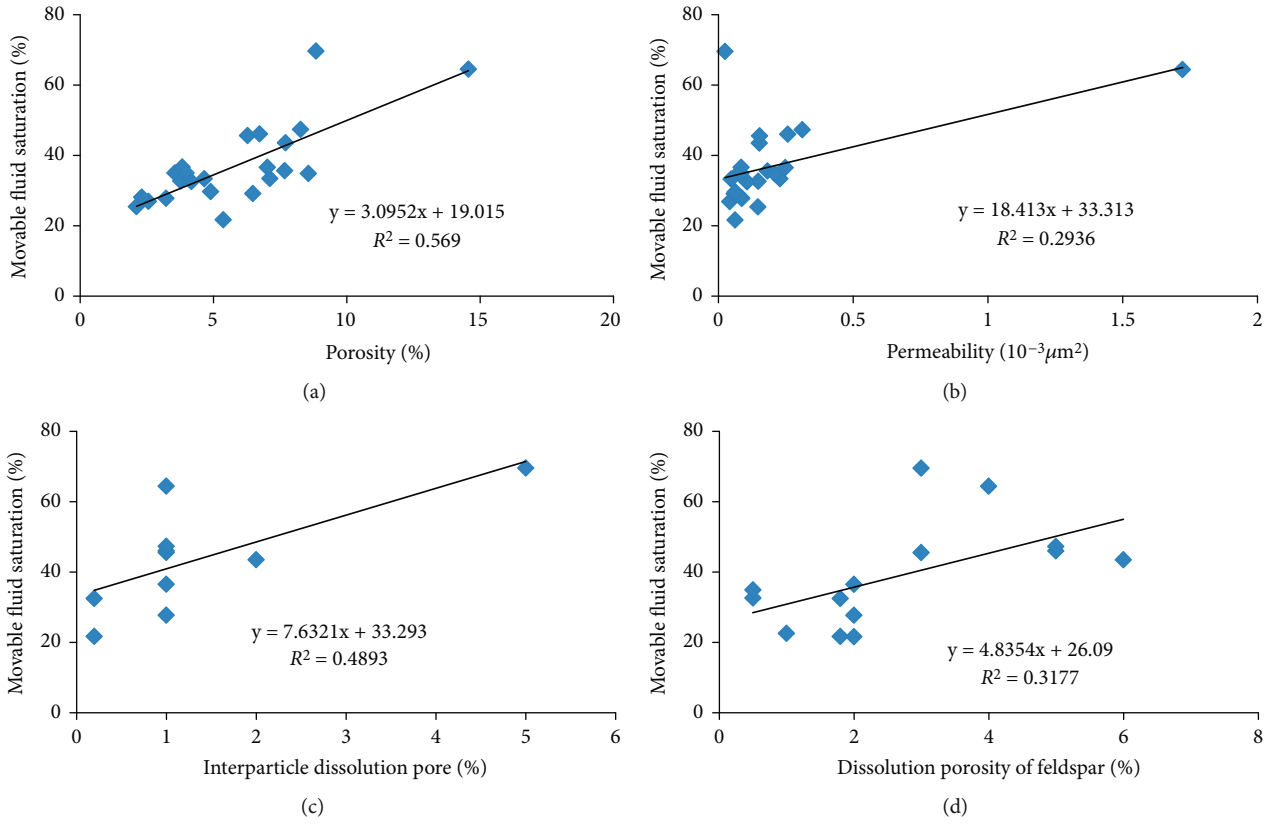


Figure 8: Reservoir physical property, pore type, and movable fluid saturation.

obvious as that of intergranular solution pores. The development of cuttings solution pores, feldspar solution pores, and intergranular pores will affect the movable fluid saturation, while the developed micropores and complex throats may have a negative effect on saturation of the movable fluid.

The relationship between maximum pore throat radius, average pore throat radius, median radius, and movable fluid saturation is shown in Figures 9(a)–9(c). There is an obvious positive relationship between maximum pore throat radius, average pore throat radius, median radius, and movable fluid saturation, and correlation coefficients are 0.7273, 0.7334, and 0.6404, respectively. The results show that the more developed the reservoir pore is, the larger the maximum pore throat radius is, the larger the average pore radius is, and the larger the median radius is, the higher the reservoir movable fluid saturation is. The reason why the maximum pore throat radius, average pore throat radius, median radius, and movable fluid saturation deviate from the positive correlation may be related to the development of microthroat. From the perspective of correlation, the main factor affecting movable fluid saturation is large pore throat, and the median radius, especially in some type II and III reservoir, is usually less than 0.1 $\mu$m and provided by nanometer pore throat less than 0.1 $\mu$m. Pores less than 0.1 $\mu$m are nanopores, while 20-50 nm is usually the lower limit of tight reservoir [28]. Combined with experimental studies, it is considered that nanopores less than 0.1 $\mu$m may be disadvantageous to fluid flow. This part of the pore throat may not be conducive to fluid flow and will increase the content of irreducible water, so the median radius has relatively little effect on saturation of movable fluid. There is a poor correlation between the homogenization coefficient and the relative sorting coefficient (Figures 9(d) and 9(e)). For tight reservoirs, the more uniform pores are, the more conducive to fluid flow, but there is still a contribution of macropores to fluid flow. Therefore, the correlation between pore uniformity and movable fluid degree is poor.

The relationship between maximum mercury saturation, displacement pressure, median pressure, and movable fluid saturation is shown in Figures 9(f)–9(h), in which the maximum inlet mercury saturation is positively correlated with movable fluid saturation, and the correlation coefficient is 0.2861. The movable fluid saturation increases with the increase of the amount of mercury in the pore throat. The results show that pores provide the main space for reservoir movable fluid. The increase of a large number of nanopore throats less than 0.1 $\mu$m is the main reason for the low correlation between maximum mercury saturation and movable fluid saturation. There is a negative correlation between displacement pressure, median pressure, and movable fluid saturation, and the correlation coefficients are 0.1727 and 0.2926, respectively, indicating that the lower the displacement pressure is, the lower the movable fluid saturation is.

*5.4. Cement.* The main cements of Shan 1 member in Yanchang area are clay minerals, carbonate, and siliceous. The content of calcite in carbonate cement is the highest.

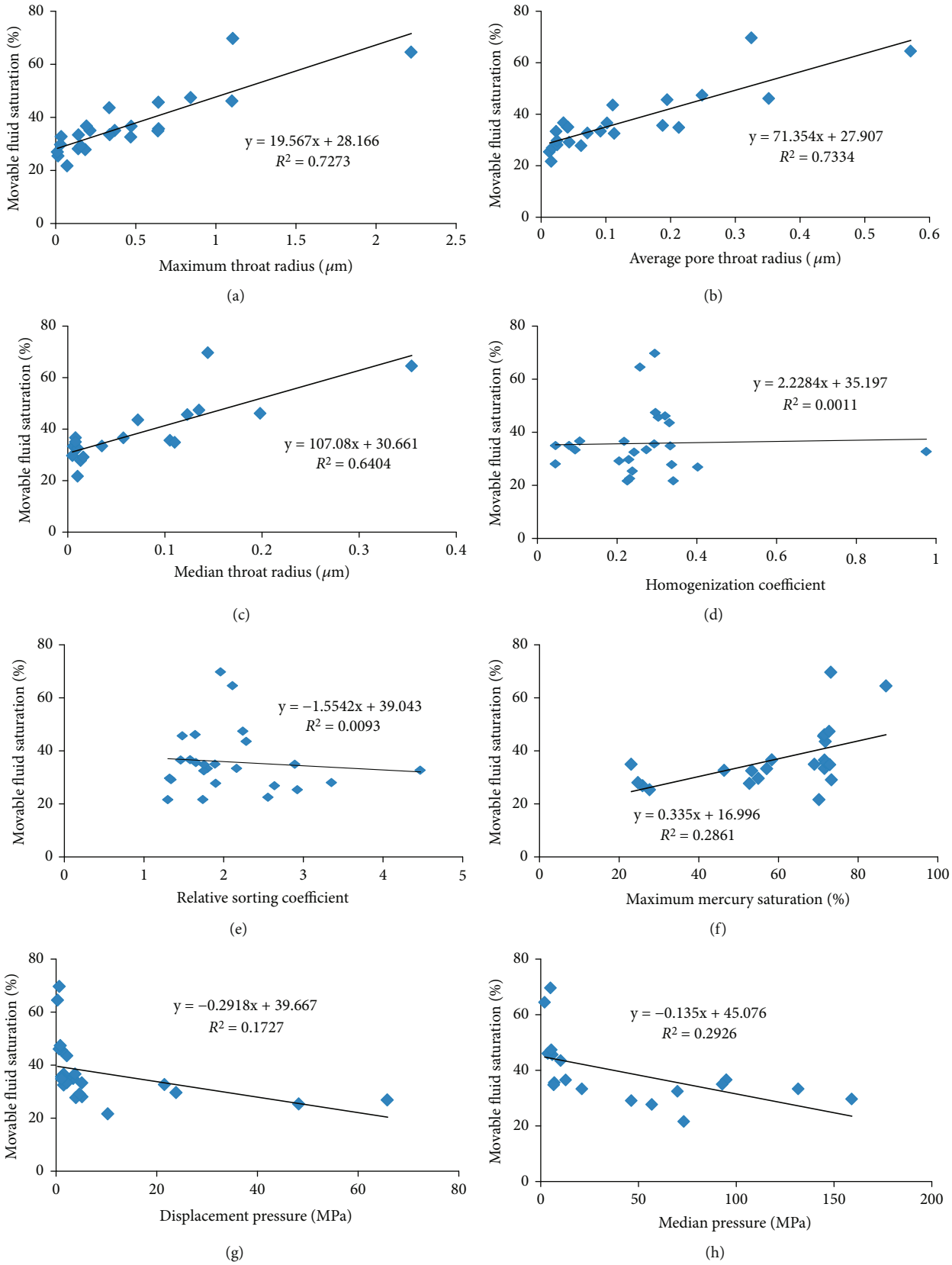


Figure 9: Reservoir pore structure parameters and movable fluid saturation.

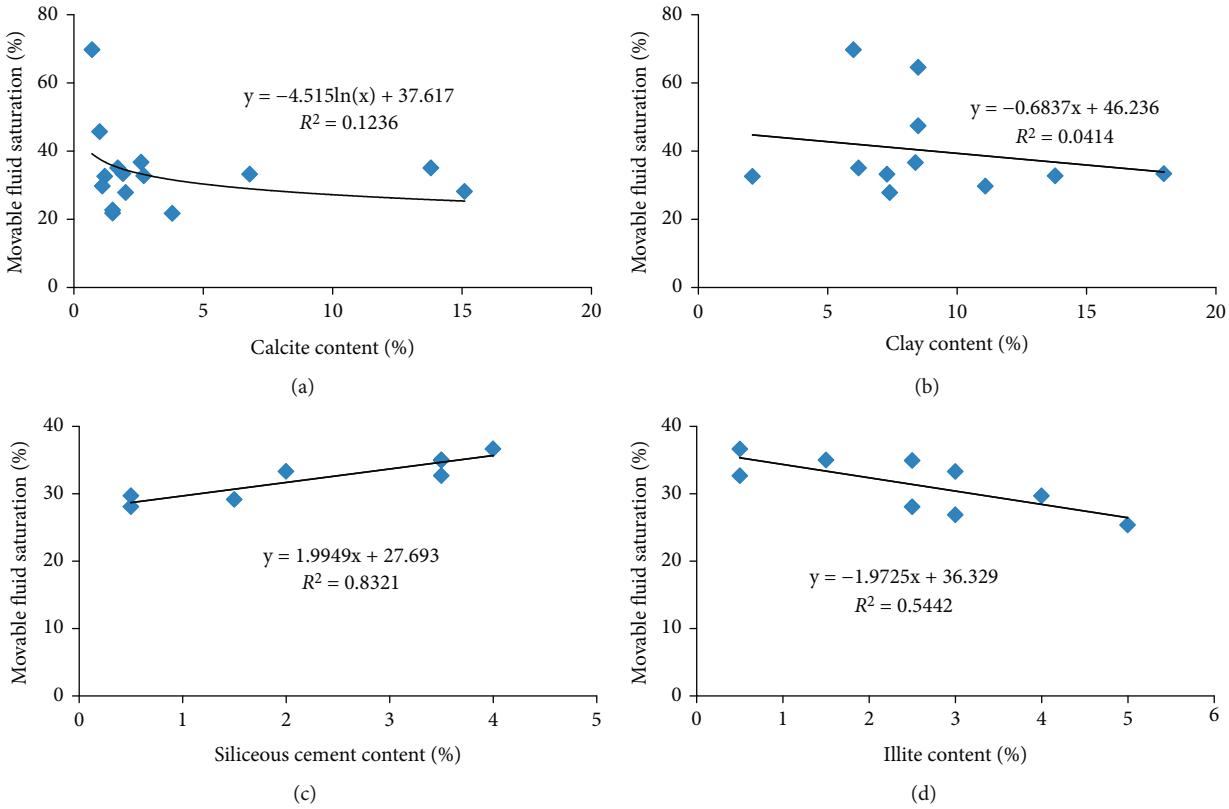


Figure 10: Reservoir cement content and movable fluid saturation.

*5.4.1. Calcite.* The relationship between calcite and movable fluid saturation is shown in Figure 10(a), showing a negative correlation; the correlation coefficient is 0.1236. The higher the calcite contents in the reservoir, the lower fluid flow property in reservoir. Thin sections show that calcite usually fills the pores with the base type, resulting in a significant reduction or even disappearance of pores. Calcite occupies the center of the pore, which makes the pore space smaller, the throat thinner, and the connectivity complex (Figures 4(g) and 4(h)). Due to the decrease of pore space, the macropores are destroyed and the pore-throat connectivity is complex, which is not conducive to fluid flow and the content of bound water increases.

*5.4.2. Siliceous.* The siliceous content is positively correlated with the movable fluid saturation (Figure 10(c)), and the correlation coefficient is 0.8321, indicating that the higher the siliceous content, the better fluid flow property in reservoir. The main reason is that the generation of siliceous particles is closely related to quartz particles, which have strong compressive properties, which are beneficial to remnant of pores [29, 30]. Quartz enlargement and authigenic quartz are common in Shan 1 reservoir (Figures 4(l) and 5(e)); both quartz enlargement and authigenic quartz will reduce intergranular pore, while authigenic quartz is mainly silicon affected by clay film, forming crystals and weakening the destruction of intergranular pores. Although the secondary enlargement of quartz and the formation of secondary quartz will lead to the reduction of pores, it is of more significance for pore preservation.

*5.4.3. Clay Minerals.* The main clay minerals in Shan 1 member of Yanchang area are illite and kaolinite. Clay mineral content has a poor effect on fluid flow property (Figure 10(b)). Types of clay minerals have different effects on movable fluid saturation. Scanning electron microscope shows that illite occurs in the shape of filamentous and occupies the pores in a disorderly form (Figure 5(b)), which is not conducive to the preservation of pores, thus hindering the flow of pore fluid. The relationship between illite content and dynamic fluid saturation is shown in Figure 8(d), showing a negative correlation. The main reason is that the filamentous output of illite reduces the reservoir space, and the increase of its content will adversely affect the fluid flow, so the lower saturation of movable fluid. Kaolinite occurs as a page (Figure 5(i)), its formation is related to feldspar dissolution, feldspar dissolution forms solution pores, and itself will reduce pore space, so its effect on fluid occurrence is complex. There is a positive correlation between kaolinite and movable fluid saturation. The effect of kaolinite on fluid flow property in reservoir has a dual nature, so it has a certain positive correlation, and the correlation coefficient is low. Kaolinite is related to the dissolution of feldspar, and its content can reflect the development of solution pores to a certain extent, but as a clay mineral, kaolinite will fill the pore space and easily form intercrystalline pore, which has a double effect on fluid flow [31, 32]. Chlorite is attached to the surface of particles in the shape of leaves (Figure 5(g)), which can prevent the secondary enlargement of quartz and is usually beneficial to the preservation of pore. The influence of chlorite on reservoir pores is more complex.

Early chlorite is beneficial to the preservation of intergranular pores, while late chlorite is disadvantageous to the development of pores. The thin section of the casting and scanning electron microscope show that the content of chlorite is low, and the role of chlorite in preserving pores is limited, and it is still dominated by pore filling, which will adversely affect the movable fluid.

## 6. Conclusion

(1) Intergranular solution pores and cutting solution pores are mainly developed in Shan 1 reservoir in Yanchang area. It is further divided into four types, and type I reservoirs are well developed

(2) The saturation value of movable fluid is 21.64%~69.62% in Shan 1 reservoir in Yanchang area, and the average is 35.32%. The $T_2$ spectrum is mainly single peak, and the saturation value of movable fluid is the highest in type I reservoir. Sandstone types, macroscopic properties, and microscopic pore property affect reservoir fluid occurrence state

(3) The cement affects the pore development and fluid flow property in reservoir. The higher the siliceous content, the better the preservation of pores and the higher fluid flow property in reservoir. The reservoir with high calcite content has obvious pore destruction, so the movable fluid saturation of this kind of reservoir is lower

## Data Availability

The experimental data used to support the findings of this study are included within the manuscript.

## Conflicts of Interest

The authors declare that they have no conflicts of interest.

## Acknowledgments

The authors acknowledge the financial support of the project (2021JQ-627) supported by the Natural Science Basic Research Program of Shaanxi Province and the project (YDBK2017-36) supported by the Doctoral Research Start-up Project of Yan'an University.

## References

[1] J. Z. Li, B. C. Guo, M. Zheng, and T. Yang, "Main types, geological features and resource potential of tight sandstone gastrin in China," *Natural Gas Geoscience*, vol. 23, no. 4, pp. 607–615, 2012.

[2] A. Jia, Y. Wei, Z. Guo, G. Wang, D. Meng, and S. Huang, "Development status and prospect of tight sandstone gas in China," *Journal of Petroleum Science and Engineering*, vol. 42, no. 1, pp. 83–92, 2022.

[3] Z. Rukai, W. Songtao, S. Ling, C. Jingwei, M. Zhiguo, and Z. Xiangxiang, "Problems and future works of porous texture characterization of tight reservoirs in China," *Acta Petrolei Sinica*, vol. 37, no. 11, pp. 1323–1336, 2016.

[4] D. Ren, L. Ma, D. Liu, J. Tao, X. Liu, and R. Zhang, "Control mechanism and parameter simulation of oil-water properties on spontaneous imbibition efficiency of tight sandstone reservoir," *Frontiers in Physics*, vol. 176, no. 10, article 829763, 2022.

[5] D. Ren, H. Zhang, Z. Wang, B. Ge, D. Liu, and R. Zhang, "Experimental study on microscale simulation of oil accumulation in sandstone reservoir," *Frontiers in Physics*, vol. 176, no. 10, article 841989, 2022.

[6] C. H. E. N. Dayou, Z. H. U. Yushuang, and X. I. A. Yong, "Application of constant-rate mercury penetration technique in description of microscopic pore space of tight sandstone reservoir: a case of the He 8 of Middle Permian Shihezi Formation in the middle of Ordos Basin," *Journal of Northwest University: Natural Science Edition*, vol. 46, no. 3, pp. 423–428, 2016.

[7] P. Zhang, J. Zhang, Q. Zhao et al., "The application of constant-rate mercury penetration technology of Chang 7 tight sandstone reservoir pore-throat space representation in Dingbian Oildom," *Journal of Northwest University: Natural Science Edition*, vol. 48, no. 3, pp. 423–430, 2018.

[8] T. Zhu, X. Qiao, and L. Zhang, "Application of constant-rate mercury intrusion in the tight sandstone reservoirs of southeastern Ordos Basin," *Special oil and gas reservoir*, vol. 26, no. 6, pp. 123–128, 2019.

[9] Y. Qu, W. Sun, R. Tao, B. Luo, L. Chen, and D. Ren, "Pore-throat structure and fractal characteristics of tight sandstones in Yanchang Formation, Ordos Basin," *Marine and Petroleum Geology*, vol. 120, article 104573, 2020.

[10] H. Huang, D. Ren, Y. Zhou, W. Sun, and D. Liu, "Characteristics of movable fluid and pore evolution of the Chang 81sandstone reservoirs of the Ordos Basin," *Journal of Northwest University: Natural Science Edition*, vol. 46, no. 5, pp. 735–745, 2016.

[11] H. Xing, L. Tiantai, W. Xiangzeng et al., "Distribution characteristics and influencing factors of movable fluid in tight sandstone reservoir- a case study from Chang 8 oil layer of Yangchang Formation reservoir in Jiyuan oilfield, Ordos Basin," *Acta Petrolei Sinica*, vol. 40, no. 5, pp. 557–567, 2019.

[12] Y. Wu, W. Sun, K. Du, P. Li, and Y. Qu, "Influence of pore-throat structure differences on occurrence characteristics of movable fluid in tight sandstone reservoirs: an example of the 8th memberof Permian Xiashihezi Formation in the east and west of the Sulige gas field," *Geology and Exploration*, vol. 55, no. 1, pp. 212–222, 2019.

[13] X. Liu, X. Dong, N. Golsanami et al., "NMR characterization of fluid mobility in tight sand: analysis on the pore capillaries with the nine-grid model," *Journal of Natural Gas Science and Engineering*, vol. 94, article 104069, 2021.

[14] Y. Pan, Z. Huang, T. Li, X. Xu, X. Chen, and X. Guo, "Pore structure characteristics and evaluation of lacustrine mixed fine-grained sedimentary rocks: a case study of the Lucaogou Formation in the Malang Sag, Santanghu Basin, Western China," *Journal of Petroleum Science and Engineering*, vol. 201, article 108545, 2021.

[15] Y. Gao, P. Li, and T. Li, "Influence of different pore structure types on the occurrence features of movable fluid in Chang-10 reservoir in Wuqi–Ansai Oilfield," *Journal of Petroleum Exploration and Production*, vol. 11, no. 4, pp. 1609–1620, 2021.

[16] P. Li, W. Sun, B. Wu, Y. Gao, and K. du, "Occurrence characteristics and influential factors of movable fluids in pores with different structures of Chang $6_3$ reservoir, Huaqing Oilfield, Ordos Basin, China," *Marine and Petroleum Geology*, vol. 97, pp. 480–492, 2018.

[17] Q. Zang, C. Liu, R. S. Awan et al., "Comparison of pore size distribution, heterogeneity and occurrence characteristics of movable fluids of tight oil reservoirs formed in different sedimentary environments: a case study of the Chang 7 member of Ordos Basin, China," *Natural Resources Research*, vol. 31, pp. 1–28, 2022.

[18] S. Wu, S. Lin, D. Chao et al., "Structure investigation in in tight sandstone: a case study of Upper Triassic Chang 6 tight sandstone in Huaqing area, Ordos Basin," *Natural Gas Geoscience*, vol. 30, no. 8, pp. 1222–1232, 2019.

[19] Z. Meng, W. Sun, Y. Liu, B. Luo, and M. Zhao, "Effect of pore networks on the properties of movable fluids in tight sandstones from the perspective of multi-techniques," *Journal of Petroleum Science and Engineering*, vol. 201, article 108449, 2021.

[20] W. H. Li, Q. Chen, Z. C. Li, R. G. Wang, Y. Wang, and Y. Ma, "Lithofacies palaeogeography of the Early Paleozoic in Ordos area," *Journal of paleogeography*, vol. 14, no. 1, pp. 85–100, 2012.

[21] Y. Guo, W. Li, B. Guo et al., "Sedimentary systems and palaeogeography evolution of Ordos Basin," *Journal of paleogeography*, vol. 21, no. 2, pp. 293–320, 2019.

[22] Y. Q. Guo, M. X. Wang, B. C. Guo et al., "Sedimentary system characteristics and paleographic evolution of Upper Paleozoic of northern west margin, Ordos Basin," *Journal of Northwest University: Natural Science Edition*, vol. 50, no. 1, pp. 93–104, 2020.

[23] M. Yao, L. Wenhou, W. Ruogu, P. Jungang, and W. Yue, "Sedimentary facies and its evolution of the Upper Palaeozoic in Zizhou area of Ordos Basin," *Chinese Journal of Geology*, vol. 50, no. 1, pp. 286–302, 2015.

[24] L. I. Weiqiang, M. U. Longxin, and Z. H. A. O. Lun, "Pore-throat structure characteristics and their impact on the porosity and permeability relationship of Carboniferous carbonate reservoirs in eastern edge of Pre-Caspian Basin," *Petroleum Exploration and Development*, vol. 47, no. 5, pp. 958–971, 2020.

[25] M. Zhao, J. Tian, X. Zhang, and B. Su, "Reservoir characteristics and main controlling factor analysis: taking Lower Permian Shanxi Formation in Shilijiahan area of North Ordos Basin as an example," *Fault-Block Oil and Gas Field*, vol. 27, no. 2, pp. 155–159, 2020.

[26] P. Li, W. Sun, C. Z. Li, Y. L. Gao, Y. Y. Bai, and D. Kun, "Characteristics of movable fluids in the low permeability sandstone reservoir: taking the Chang 8 reservoir of Maling oilfield, Ordos basin as an example," *Progress in Geophysics*, vol. 33, no. 6, pp. 2394–2402, 2018.

[27] J. Zhou, X. Qiao, R. Wang et al., "Effective reservoir development model of tight sandstone gas in Shanxi Formation of Yan'an Gas Field, Ordos Basin, China," *Journal of Natural Gas Geoscience*, vol. 7, no. 2, pp. 73–84, 2022.

[28] L. Sun, H. Xiao, L. Tan, B. Li, D. Sun, and P. Wang, "Pore structure comparison and difference mechanism between tight sandstone and tight conglomerate reservoirs," *Acta Geologica Sinica*, vol. 96, no. 6, pp. 2155–2172, 2022.

[29] P. Guo, H. Qu, H. Yang, X. Tian, W. Dong, and Y. Chen, "Characteristics of cement and its influence on reservoir physical properties of Shan 2 member of Shanxi Formation in the east of Ordos Basin," *Geological science and technology information*, vol. 36, no. 2, pp. 51–57, 2017.

[30] H. Ju, W. Sun, X. Yang, and Z. Han, "Reservoir characteristics and main controlling factors of P1s2 member in Yan'an area, Ordos Basin," *Fault block oil & gas field*, vol. 18, no. 2, pp. 142–145, 2011.

[31] Q. Wan, A. P. Fan, R. C. Yang, and N. Lenhardt, "Diagenetic mineralogy and its effect on the reservoir properties of the sandstones of the Permian of S120 block (Sulige gas field), Ordos Basin, NW China," *Journal of Paleogeography*, vol. 11, no. 3, pp. 360–386, 2022.

[32] B. Jiu, W. Huang, Y. Li, and M. He, "Influence of clay minerals and cementation on pore throat of tight sandstone gas reservoir in the eastern Ordos Basin, China," *Journal of Natural Gas Science and Engineering*, vol. 87, article 103762, 2021.